Rolling Bearing Reliability Prediction Based on Signal Noise Reduction and RHA-MKRVM

Yifan Yu
School of Information and Computer Science, Nantong Institute of Technology, Nantong, Jiangsu, PR China

***Abstract*—In order to solve the problem of reliability assessment and prediction of rolling bearings, a noise reduction method (CEEMDAN-GRCMSE) based on complete ensemble empirical mode decomposition with adaptive noise(CEEMDAN) combined with generalized refined composite multi-scale sample entropy (GRCMSE) is proposed from the vibration signals to remove the noise from the bearing vibration signals, and then the feature set of the noise-reduced signals is downscaled by using the Uniform manifold approximation and projection(UMAP) algorithm, and the reliability assessment model is established by using a logistic regression algorithm to establish a reliability assessment model, and use the red-tailed hawk algorithm for parameter optimization of the mixed kernel relation vector machine, which is used to predict the bearing state, and finally the predicted state information is brought into the assessment model to obtain the final results. In this paper, the whole life cycle data of rolling bearings from Xi 'an Jiaotong University-Sun Science and Technology Joint Laboratory (XJTU-SY) are used to verify the effectiveness of the proposed method. The superiority of the proposed method is highlighted by comparing the analysis results with those of other AI methods.**

Keywords*—Rolling bearing; reliability evaluation and prediction; complete ensemble empirical mode decomposition with adaptive noise; generalized refined composite multi-scale sample entropy; uniform manifold approximation and projection; red-tailed hawk algorithm; mixed kernel relevance vector machine

I. Introduction

With the evolution of mechanical equipment to intelligentization, an in-depth understanding of the degradation law of equipment components becomes the key to ensure its stable operation [1]. As an indispensable core component of mechanical systems, the performance state of rolling bearings has a decisive influence on the stable operation of the whole equipment [2]. Therefore, it is particularly important to carry out effective reliability assessment and prediction [3]. However, in practical engineering applications, the operation of mechanical equipment is inevitably accompanied by the generation of various noise signals. The existence of these noises seriously interferes with the accurate monitoring and assessment of the bearing state, thus affecting the accurate judgment of the bearing health state. Therefore, the removal of rolling bearing noise and vibration signals has a very important role in the extraction of effective information extraction of bearings. Traditional signal processing methods such as Fourier transform [4], wavelet packet transform (WPT) [5], etc., are mostly centered around the wavelet basis of the signal, and it is easy for the signal to be over-decomposed. Based on these limitations, Adaptive Mode Decomposition (AMD) is widely used due to its ability to analyze complex signals [6] [7] [8].

Complete Ensemble Empirical Mode Decomposition with Adaptive Noise (CEEMDAN) [12] is an adaptive signal processing method based on Empirical Mode Decomposition (EMD) and its deformations [9] [10] [11], which effectively improves the stability and robustness of the decomposition by the method of adding random noise to the original signal. Cheng et al. [13] used CEEMDAN to analyze the bearing signals, adding Gaussian noise adaptively at each stage of the signal decomposition to completely decompose the signal, which greatly improved the accuracy of rolling bearing fault diagnosis. Kala A et al. [14] established a rainfall prediction model based on CEEMDAN combined with a long and short term memory network (LSTM), which greatly improved the climate change rainfall prediction accuracy due to climate change. Li H [15] proposed a CEEMDAN-SVD-TE based vibration signal analysis method to solve the problem of complex vibration sources in hydropower stations, which improves the accuracy of vibration propagation path identification. Zhao et al. [16] proposed a CEEMDAN based ECG signal elimination method to filter out high frequency noise. D et al. [17] proposed a CEEMDAN combined with health indicator screening and Gray Wolf Optimized Extreme Learning Machine (GWO-ELM) for the prediction of remaining useful life (RUL) of lithium-ion batteries. Noise reduction of battery signals by CEEMDAN effectively improves the signal quality.

Reliability refers to the ability to fulfill a predetermined function within a certain period of time [18]. Rolling bearing reliability assessment usually starts from the characteristics of the vibration signals and collects effective information by extracting multiple features from the signals to assess the bearing reliability. Logistic Regression (LR) is a mathematical modeling method that is often used to model the reliability assessment of bearings. Gao et al. [19], in order to solve the problem of assessment and prediction of the operational reliability of rolling bearings, proposed a method based on isometric mapping, logistic regression modeling, and Nonhomogeneous Cuckoo algorithm-Least Squares Support Vector Machine (NoCuSa-LSSVM) for the prediction of the operational reliability of rolling bearings. Abbasi et al. [20] used Logistic regression model to check and evaluate iot anomalies, and achieved good results.

With the rapid development of artificial intelligence, prediction methods based on machine learning have gradually become an important means in the field of reliability prediction. In the process of reliability prediction, the characteristics of the bearings are first analyzed, and the degradation state of the bearings is predicted by machine learning methods. From then on, the degradation states obtained from these predictions are used as inputs for reliability calculations using reliability assessment models. Li et al. [21] proposed a hybrid

prediction algorithm to predict the bearing degradation trend by combining a Sparse Low-Rank Matrix (SLRM) with a Chaos Cuckoo Search (CCS) optimized support vector machine model. Han et al. [22] used a stacked self-encoder combined with a long short-term memory network model to establish a bearing degradation state prediction model and analyze the remaining service life of the bearings. Wang Y et al. [23] proposed a method based on Pearson correlation coefficient and kernel principal component analysis (KPCA) for the prediction of the remaining service life of rolling bearings. Xu et al. [24] established an (MSMHA-AED) model to predict the degree of bearing degradation. Bo et al. [25] proposed an adaptive temporal convolutional network (TCN) based on improved SSD and correlation coefficient (ISSD-CC) for bearing condition prediction.

Through the comprehensive analysis of the existing literature, it can be found that although various noise reduction techniques are adopted, these methods still have the problems of low efficiency and poor noise reduction effect when dealing with complex vibration signal noise. To overcome these challenges, a noise reduction method based on adaptive noise based complete ensemble empirical Mode decomposition (CEEMDAN) and generalized fine composite multi-scale sample entropy (CEEMDAN-GRCMSE) is proposed in this paper. Firstly, a series of intrinsic mode functions (IMFs) are obtained by CEEMDAN decomposition of noisy vibration signals. Then, by calculating the GRCMSE value of each component, the most representative modal component is selected from a large number of IMFs, which lays the foundation for the subsequent signal processing. In addition, in order to improve the accuracy of rolling bearing reliability prediction, a hybrid kernel relational vector machine (MKRVM) parameter optimization method combined with Red Tail Eagle optimization algorithm (RHA) was proposed and applied to bearing reliability evaluation and prediction. Using RHA algorithm to optimize the parameters of MKRVM, the performance of the prediction model can be significantly improved. The main innovations are:

1. For the selection of IMFs after CEEMDAN decomposition, combined with GRCMSE, the efficiency and accuracy of over-signal noise reduction are improved.

2. In the reliability modeling process of rolling bearings, the uniform manifold approximation and projection (UMAP) algorithm is used to reduce the order of the multi-dimensional features of the signal after noise reduction. Compared with other order reduction algorithms, UMAP algorithm can retain as much information in the data as possible, thus laying a solid data foundation for the reliability modeling of rolling bearings.

3. Aiming at the problem of bearing reliability prediction, MKRVM model optimized by RHA is proposed to predict the reliability of bearing signals, which significantly improves the prediction accuracy.

The structure of this paper is as follows: the first section is the introduction, the second section introduces the CEEMDAN-GRCMS signal noise reduction model, the third section introduces the establishment of the logistic regression bearing reliability model based on data characteristics, the fourth section introduces the rham-mkrvm model, the fifth section verifies the model experimentally, and the sixth section summarizes the conclusions of this paper.

II. Noise Reduction of the Vibration Signal

A. CEEMDAN

Complete Ensemble Empirical Mode Decomposition with Adaptive Noise (CEEMDAN) is a mode decomposition algorithm. CEEMDAN introduces an adaptive Gaussian white noise and effectively maintains the signal integrity. In addition, the time complexity of the traditional algorithm is significantly reduced and the efficiency is improved. The main steps as follows:

Step 1: Add pairs of positive and negative Gaussian white noise $\lambda^i(t)$ to the original signal to obtain $x^{\,i}(t) = x(t) + \lambda^{\,i}(t)$, decompose $x^{\,i}(t)$ to obtain the 1st modal component (IMF) and take its mean value as the 1st IMF obtained by CEEMDAN decomposition,and a residual component $r_1(t)$.

$$I_{\text{IMF1}} = \frac{1}{n}\sum_{i=1}^{n} I^i_{\text{IMF1}}(t) \tag{1}$$

$$r_1(t) = x(t) - I_{\text{IMF1}} \tag{2}$$

where ${IMF_1}^i(t)$ represents the 1st modal component; n is the number of signals.

Step 2: Add pairs of positive and negative Gaussian white noise $\lambda^i(t)$ to the first residual component $r_1(t)$ to obtain a new component $r^{\,i}{}_1(t) = r_1(t) + \lambda^i(t)$. Perform the EMD decomposition of this component again, the process is calculated as follows:

$$I_{\text{IMF2}} = \frac{1}{n}\sum_{i=1}^{n} \text{EMD}(r_1(t) + \lambda^i(t)) \tag{3}$$

$$r_2(t) = r_1(t) - I_{\text{IMF2}}(t) \tag{4}$$

Step 3: Repeat the decomposition until the resulting residual signal can no longer be decomposed (the number of extreme points is no more than 2). Finally, $I_{\text{IMF1}}\, I_{\text{IMF2}} \cdots I_{\text{IMF}n}$ can be obtained in turn for the corresponding residual components. The original signal can be expressed as:

$$x(t) = \sum_{j=1}^{q} I_{\text{IMF}j} + r_z(t) \tag{5}$$

where q is the total number of modes after decomposition and $r_z(t)$ is the final residual result.

B. Generalized Refined Composite Multi-scale Sample Entropy

Generalized Refined Composite Multi-scale Sample Entropy (GRCMSE) is an improved algorithm developed on the basis of Sample Entropy (SE) [26]. Sample entropy is a quantitative measure of the degree of chaos in a time series, and the magnitude of its value is proportional to the irregularity and noise content of the time series. A high sample entropy value usually indicates that the signal has a high level of irregularity and noise.GRCMSE introduces a variance coarse-graining method to enhance the extraction of data information and improve the algorithm's resistance to noise. This enables GRCMSE to provide more accurate and reliable results when dealing with signal and data analysis in complex environments. In GRCMSE, a larger entropy value means that the signal

contains more valid information.The calculation procedure of GRCMSE is as follows:

Step1: For the time series x(i),i=1,2,3... ,n. Firstly, the original time series x(i) is coarsely granulated, and for the scale factor τ the corresponding coarsely granulated sequence can be expressed as $\mathrm{y_{g,h}}^{\tau}$

$$\mathrm{y_{g,k,j}}^{\tau} = \frac{1}{\tau} \sum_{i=(j-1)\tau+k}^{j\tau+k-1} (x_i - \overline{x_i})^2 \tag{6}$$

where $1 \leq j \leq \frac{N}{\tau}$, $2 \leq k \leq \tau$, $\overline{x_i} = \frac{1}{\tau} \sum_{k=0}^{\tau-1} x_{i+k}$

Step2: For the scale factor τ, compute the number of vectors $\mathrm{y_{g,h}}^{\tau}$ in the t-dimensional as well as t+1-dimensional space for each generalized coarse-grained sequence under this scale factor, denoted respectively as $\mathrm{n_{g,h,s}}^{t}$ and $\mathrm{n_{g,h,s}}^{t+1}$.

Step3: Calculate the average of $\mathrm{n_{g,h,s}}^{t}$ and $\mathrm{n_{g,h,s}}^{t+1}$ in the range $1 \leq h \leq \tau$,the generalized fine composite multiscale sample entropy of the initial time series x(i) under the scale factor τ can be obtained as:

$$E_{GRCMSE} = -\ln(\frac{\overline{n_{g,h,\tau}}^{t+1}}{\overline{n_{g,h,\tau}}^{t}}) \tag{7}$$

$$\overline{n_{g,h,\tau}}^{t} = \frac{1}{\tau} \sum_{h=1}^{\tau} {n_{g,h,\tau}}^{t} \tag{8}$$

$$\overline{n_{g,h,\tau}}^{t+1} = \frac{1}{\tau} \sum_{h=1}^{\tau} {n_{g,h,\tau}}^{t+1} \tag{9}$$

III. Rolling Bearing Reliability Model

A. UMAP Dimensionality Reduction

Uniform manifold approximation and projection (UMAP) [27] is a powerful dimensionality reduction algorithm based on Riemannian geometry and algebraic topology. The core advantage of UMAP is that it can retain the global structure and local features of data more effectively. Compared with the traditional Principal Component Analysis (PCA) [28], UMAP can retain more data information in the dimensionality reduction process. UMAP shows faster computing speed and better performance. The specific implementation process of UMAP consists of two phases, namely, learning the flow structure in the high-dimensional space and making a low-dimensional representation of the flow structure.

Assuming that $X = \{x_1, x_2, ..., x_N\}$ is the original N-dimensional dataset, in the first stage, the main task is to create a weighted k-neighborhood graph G=(V,E,W). Where V is the set of vertices consisting of the original N-dimensional data, E denotes the set of edges, i.e., the set of directed edges that can be formed according to the k neighboring points, and W is the weight function, which is computed by the equation.

$$W_{ij} = \mathrm{e}^{-\frac{s_{ij}+\varepsilon_i}{\tau_i}} \tag{10}$$

where $\mathrm{s_{ij}}$ denotes the distance between $\mathrm{x_i}$ and $\mathrm{x_j}$; ε_i denotes the distance between $\mathrm{x_i}$ and its neighboring points; and τ_i is the smoothing normalization factor set according to the Riemannian metric. By calculating the weight values of all data points, a weighted near proximity graph of the high-dimensional dataset can be generated G. In order to ensure that the weights between data points are consistent, the expression is introduced:

$$T = A + A^{\mathrm{T}} - A \circ A^{\mathrm{T}} \tag{11}$$

where T is the adjacency matrix of the weighted nearest neighbor graph G, A is the weighted adjacency matrix consisting of the weight values $\mathrm{W_{ij}}$, and $\circ$ denotes the Hadamard product of the sought matrix.

After completing the construction of the high-dimensional structure, the next step is to map it to the low-dimensional space. Firstly, the weight function in low dimensions needs to be constructed with the mathematical formula:

$$V_{ij} = \frac{1}{1+ac_{ij}^{2b}} \tag{12}$$

where a and b denote hyperparameters and $\mathrm{c_{ij}}$ is the distance between $\mathrm{y_i}$ and $\mathrm{y_j}$ in the data point $Y = \{y_1, y_2, ..., y_N\}$ in the low-dimensional space.

In order to make the dimensionality reduced dataset as close as possible to the original dataset, it can be optimized by minimizing the cross-entropy loss between $\mathrm{Y_{ij}}$ and $\mathrm{T_{ij}}$. The cross-entropy function is:

$$L_{\mathrm{c}} = \sum_{ij} [T_{ij} \log \frac{T_{ij}}{V_{ij}} + (1 - T_{ij}) \lg \frac{1-T_{ij}}{1-V_{ij}}] \tag{13}$$

In the above equation, the first term is the attraction component, which is used to constrain the clusters formed by similar data points, and the second term is the repulsion component, which is used to ensure that the clusters formed have a sufficiently large interval between them. The stochastic gradient descent algorithm can be used to optimize the cross-entropy function, and after obtaining the weights of the low-dimensional data points, the construction of the weighted nearest-neighbor graph in low dimensions is completed, and ultimately the low-dimensional representation of the high-dimensional topology is completed, so as to achieve the effect of data dimensionality reduction.

B. Logistic Regression Model

Logistic regression model [29] can give the probability of an event occurring under a series of characteristic parameters, is a linear regression model built on a large amount of data, and is now widely used in statistics, medicine, and economics. The logistic regression model is often used to deal with binary classification problems. The model essentially consists of a linear regression and a sigmoid function. The logistic regression model obtains the corresponding output value through the sigmoid function, which is shown in Fig. 1:

Assuming that the i-th dimension feature parameter set at moment t is $X_i(t) = (\mathrm{x_1}(t), x_2(t), \ldots, x_i(t))$, the normal operation of the bearing at the moment is denoted as $y(t) = 1$. The set of characteristic parameters is entered into the sigmoid

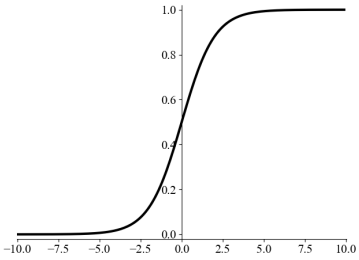

Fig. 1. Sigmoid function.

function and the bearing reliability R is calculated by the following equation:

$$R = P\left(y_i = 1 \mid X_i\right) = \frac{\exp(\theta_0+\theta_1 x_1(t)+\theta_2 x_2(t)+\ldots+\theta_i x_i(t))}{1+\exp(\theta_0+\theta_1 x_1(t)+\theta_2 x_2(t)+\ldots+\theta_i x_i(t))} \tag{14}$$

where $\theta_0, \ldots\ldots\theta_i$ is the regression coefficient for the set of eigenvectors. This coefficient is similar to the linear regression coefficient, which represents the change of the dependent variable due to the change of the independent variable. Logistic regression model regression coefficient is solved using the maximum likelihood estimation method. First, the above equation is transformed:

$$\ln \frac{P(y_i=1|X_i)}{1-P(y_i=1|X_i)} = \theta_0 + \theta_1 x_1(t) + \theta_2 x_2(t) + \ldots + \theta_i(t) \tag{15}$$

Setting $R = \theta_0, \ldots\ldots\theta_i$ to be brought into the above equation gives:

$$lnL(R) = \textstyle\sum_i [y_i RX(t) - \ln(1 + \exp(RX(t)))] \tag{16}$$

Then the gradient descent method is used to solve the above equation, the regression coefficients of the set of feature vectors can be obtained, and the regression coefficients are brought into the reliability solving formula to establish a logistic regression reliability assessment model.

IV. Reliability Prediction of Rolling Bearing

A. Red-tailed Hawk Algorithm

Red-tailed hawk algorithm (RTH) [30] is a meta-heuristic algorithm proposed in 2023. The optimization process of this algorithm simulates the hunting behavior of red-tailed hawk and has the advantage of high search efficiency. The hunting process of red-tailed hawk is divided into three phases,which are: high soaring, low soaring and swooping phase. In the high-altitude soaring stage, the red-tailed hawk spreads its wings and flies, using its sharp vision to scan the vast field and determine the exact location of the prey. Subsequently, the low-altitude soaring phase allows for a more careful examination of the ground and a gradual approach to the previously identified prey area. After determining the optimal location of the prey, the red-tailed hawk enters a phase of sharp turns and dives, quickly swinging its wings, adjusting its flight position, and getting ready to execute the hunting action to rapidly approach the prey. The general steps of the red-tailed hawk optimization algorithm are:

1) Initialize population: Map the solution space of the problem to the hunting domain of the red-tailed hawk and generate a group of possible solutions as the initial population.

2) High flying phase: The red-tailed hawk will take to the skies in search of the best location for food supply. The mathematical model for the high flight phase of the red-tailed hawk is:

$$X(t) = X_{\text{best}} + (X_{\text{mean}} - X(t-1)) \cdot Levy(\text{dim}) \cdot TF(t) \tag{17}$$

where, t is the number of iterations, X (t) denotes the red-tailed hawk position for t iterations, $\mathrm{X_{best}}$ is the best position obtained,$\mathrm{X_{mean}}$ is the average of the red-tailed hawk positions, and Levy values can be calculated based on the distribution function formula for Levy flights, which is given below:

$$Levy(\text{dim}) = s\frac{\mu\cdot\sigma}{|v|^{\beta-1}} \tag{18}$$

$$\sigma = \frac{\Gamma(1+\beta)\cdot\sin(\pi\beta/2)}{\Gamma(1+\beta/2)\cdot\beta\cdot 2^{(1-\beta/2)}} \tag{19}$$

where, s is a constant (0.01), dim is the dimension of the problem, β is a constant (1.5), and μ, ν are random numbers between 0 and 1. TF (t) can be computed based on the transition factor function with the following formula:

$$TF(t) = 1 + \sin\left(2.5 + (t/_{T_{\max}})\right) \tag{20}$$

where T_{max} denotes the maximum number of iterations.

Low-flying phase: The red-tailed hawk gradually approaches its prey using spiral flight. Its model can be expressed as follows:

$$X(t) = X_{best} + (x(t) + y(t)) \cdot \text{StepS}(t) \tag{21}$$

$$\text{StepS}(t) = X(t) - X_{mean} \tag{22}$$

where x and y represent the direction coordinates of the red-tailed eagle at this moment, the spiral flight method is calculated as follows:

$$\begin{aligned} x(t) &= R(t) \cdot \sin\left(\theta(t)\right) \\ y(t) &= R(t) \cdot \cos\left(\theta(t)\right) \end{aligned} \tag{23}$$

$$\begin{aligned} R(t) &= R_0 \cdot \left(r - \tfrac{t}{T_{\max}}\right) \cdot \text{rand}() \\ \theta(t) &= A \cdot \left(1 - \tfrac{t}{T_{\max}}\right) \cdot \text{rand}() \end{aligned} \tag{24}$$

$$\begin{aligned} x(t) &= \tfrac{x(t)}{\max|x(t)|} \\ y(t) &= \tfrac{y(t)}{\max|y(t)|} \end{aligned} \tag{25}$$

where R_0 represents the initial value of the radius, A represents the angular gain, taking values between 5 and 15,

rand is a random number between 0 and 1, and r represents the control gain, taking values between 1 and 2.

Sharp turn and dive phase: in this phase, the red-tailed hawk occupies the best swooping position obtained from the low altitude flight phase and prepares to attack the prey. The mathematical model for this phase is as follows:

$$X(t) = \alpha(t) \cdot X_{best} + x(t) \cdot \mathrm{StepS1}(t) + \mathrm{y}(t) \cdot \mathrm{StepS2}(t) \tag{26}$$

Each of these steps can be calculated as follows:

$$\begin{array}{c} \mathrm{StepS1}(t) = X(t) - TF(t) \cdot X_{mean} \\ \mathrm{StepS2}(t) = G(t) \cdot X(t) - TF(t) \cdot X_{best} \end{array} \tag{27}$$

where α and P are the acceleration and gravity coefficients, respectively, can be simplified as follows:

$$\begin{array}{c} \alpha(t) = \sin^2\left(2.5 - {}^{t}/_{T_{\max}}\right) \\ P(t) = 2 \cdot \left(1 - {}^{t}/_{T\max}\right) \end{array} \tag{28}$$

where α denotes that the acceleration of the hawk increases with the number of iterations to improve the convergence rate, and P is the gravitational effect that reduces the exploitation diversity as the hawk gets closer to its prey.

The high-flying phase, based on Levy flight, successfully avoids trying to fall into local minima, and the low-altitude search phase focuses on localized search to improve the accuracy of the solution. The sharp turn and dive phases adopt a more focused search strategy that enhances the accuracy of the RTH. The advantage lies in the fact that its combined global and local search strategy is able to efficiently find the global optimal solution in the solution space.

B. Relevance Vector Machine

Relevance Vector Machine (RVM), proposed by Tipping [31], is a kernel sparse machine learning method based on Bayesian framework. In the machine learning process, the sample used for training consists of an input $\{x_n\}^N$ and a target value $\{t_n\}^N$. The correspondence between the input and the target value in RVM can be expressed as:

$$t(x, \delta) = \sum_{i=1}^{N} \delta_i K(x, x_i) + \varepsilon \tag{29}$$

where δ is the weight vector of the model, K represents the kernel function, ε is the offset, and N is the total number of training samples.

Let $\{t_n\}^N$ be an independent variable, then the conditional probability of the target value can be expressed as:

$$P\left(t \mid \delta, \sigma^2\right) = \left(2\pi\sigma^2\right)^{-\frac{N}{2}} \exp\left(-\frac{\|t - \Phi\delta\|^2}{2\sigma^2}\right) \tag{30}$$

where Φ is the matrix consisting of kernel functions and σ^2 is the noise variance.

In the process of calculation, due to a large number of hyperparameters are quoted, the direct use of maximum likelihood estimation method to find the value of δ, there may be the generation of overfitting, in order to solve this problem, the application of the knowledge of Bayesian theory, add a constraint on δ, each weight vector δ is defined as a vector of zero mean, then its Gaussian prior probability distribution formula is as follows:

$$P(\delta|\alpha) = \sum_{i=0}^{N} N\left(\delta_i|0, \alpha_i^{-1}\right) \tag{31}$$

where the weight vectors are all independently distributed, $\alpha = [\alpha_0, \alpha_1, \ldots, \alpha_N]^T$ denotes the hyperparameter vector, and each hyperparameter corresponds to a weight vector. The size of hyperparameters can affect the sparsity of the model. Therefore, the key of RVM is to find the hyperparameters, find the corresponding weights and kernel function, so that the sparsity of the model is guaranteed, and combined with the noise variance, the final regression model is obtained.

The posterior distribution weights of the weight vector δ are derived from the Bayesian formula:

$$P(\delta|\alpha) = \sum_{i=0}^{N} N\left(\delta_i|0, \alpha_i^{-1}\right) \tag{32}$$

where is $\Sigma = \left(\sigma^{-2}\Phi^T\Phi + C\right)$ covariance matrix, $\mu = \sigma^{-2}\sum \Phi^T t$ is the posterior matrix of the target value, and C denotes the matrix whose main diagonal element is $\alpha = [\alpha_0, \alpha_1, \ldots, \alpha_N]^T$.

In the calculation process, in order to harmonize the hyperparameters, the definition:

$$P\left(t \mid \alpha, \sigma^2\right) = \left(2\pi\sigma^2\right)^{-\frac{N}{2}} |E|^{-\frac{1}{2}} \exp\left\{-\frac{1}{2}t^T E^{-1} t\right\} \tag{33}$$

where $E = \sigma^2 I + \Phi C^{-1}\Phi^T$, the hyperparameters α and σ^2 of the RVM are solved by an iterative algorithm as follows:

$$\alpha_i{}^{new} = \frac{1 - \alpha_i M_{ii}}{\mu_i^2} \tag{34}$$

$$\left(\sigma_i^2\right)^{new} = \frac{\|t - \Phi\mu\|^2}{N - \sum_i (1 - \alpha_i M_{ii})} \tag{35}$$

where M_{ii} is the ith diagonal element of the covariance matrix. The hyperparameters α and σ^2 are calculated iteratively by the above equation until the condition of convergence is satisfied.

In machine learning by correlation vector machines, the kernel function is a crucial part of the algorithm. The kernel function is capable of mapping nonlinear data into a high dimensional space. However, different settings of kernel function and kernel parameters affect the performance of the RVM model. Therefore, it is necessary to choose the appropriate kernel function and also optimize the kernel function parameters. Common kernel functions include Linear Kernel, Gaussian Kernel, Laplace Kernel and so on.

(1) Linear kernel function is a global kernel function.

$$k\left(x_i, x_j\right) = x_i \bullet x_j \tag{36}$$

(2) Gaussian kernel function Gaussian kernel function has strong localization, which can map the input vector to a space of larger dimensions.

$$k\left(x_i, x_j\right) = \exp\left(-\frac{\|x_i - x_j\|^2}{2\delta^2}\right) \tag{37}$$

(3) Laplace kernel function The Laplace kernel function can be seen as a variant of the Gaussian kernel function, both belong to the radial basis kernel function (RBF function).

$$k\left(x_i, x_j\right) = \exp\left(-\frac{\|x_i - x_j\|}{\delta}\right) \tag{38}$$

Different kernel functions have their own strengths and weaknesses, in order to make the model have better performance, hybrid kernel functions can be used so that the combined kernel function has the characteristics of global and local kernel to improve the ability of machine learning model. The process of optimizing the hybrid kernel correlation vector machine model using the red-tailed hawk algorithm is shown in Fig. 2:

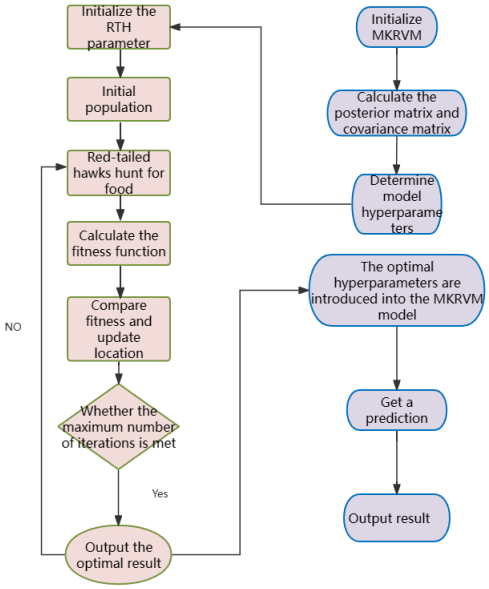

Fig. 2. RTH-MKRVM flowchart.

V. Experimental Verification

A. Experimental Data

The life cycle data of the bearings in this experiment were provided by XJTU-SY-Bearing Datasets, a bearing experiment set of Xi'an Jiaotong University. The test equipment includes AC motors, motor speed controllers, support bearings, and test bearings. A PCB352C33 transducer was placed in the horizontal and vertical directions of the bearing to collect vibration signals. A total of 32,768 data points were recorded during the first 1.28 s in 1 min. The test rig is shown in Fig. 3. Since the radial force was applied in the horizontal direction, the vibration signals in this direction were chosen for the experiment to better represent the bearing degradation.

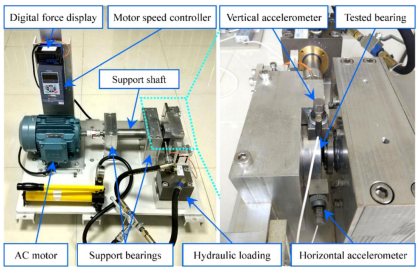

Fig. 3. Bearing test stand.

B. Experimental Procedure

The flowchart of the experiments in this paper is shown in Fig. 4 below:

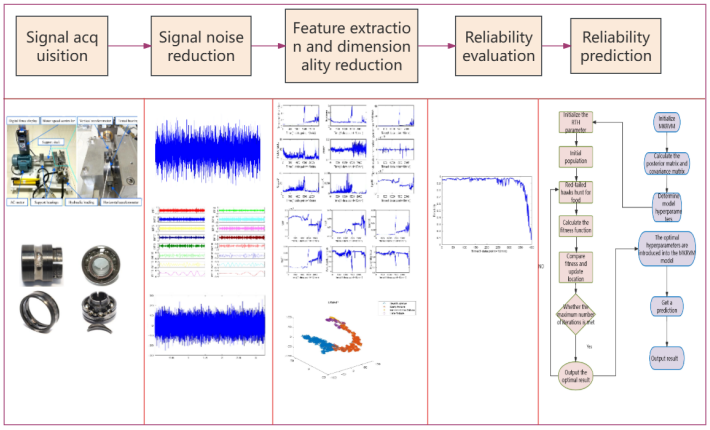

Fig. 4. Flow chart of the experiment.

C. CEEMDAN-GRCMSE Model

In order to verify the effectiveness of the proposed CEEMDAN-GRCMSE algorithm, the horizontal direction data of bearing 3-2 in the rolling bearing full-life dataset of Xi'an Jiaotong University is selected as the experimental data in Fig. 5. The performance and effectiveness of CEEMDAN-GRCMSE method will be verified by processing and analyzing the experimental data.

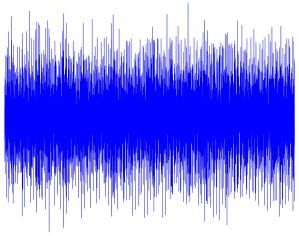

Fig. 5. Original Signal

Firstly, CEEMDAN decomposition of the noise signal is performed to obtain 16 IMF components as shown in Fig. 6, next, the GRCMSE value of each component is derived as shown in Table I. From the table, it can be seen that the front IMF components have larger values, indicating that the IMF components contain more valid information. Therefore, the IMF component with a value greater than 1 is selected and it is reconstructed. The reconstructed signal is shown in Fig. 7.

From the figure, it can be seen that the signal after CEEMDAN-GRCMSE denoising has less burrs than the original signal and the signal trend is smoother. Generally, signal-to-noise ratio (SNR) is used to indicate the size of the noise. Higher SNR values indicate better signal quality and vice versa. By calculation, the SNR of the original signal is -4.98

and the SNR of the denoised signal is -2.19. It shows that the use of CEEMDAN-GRCMSE can effectively reduce the signal noise.

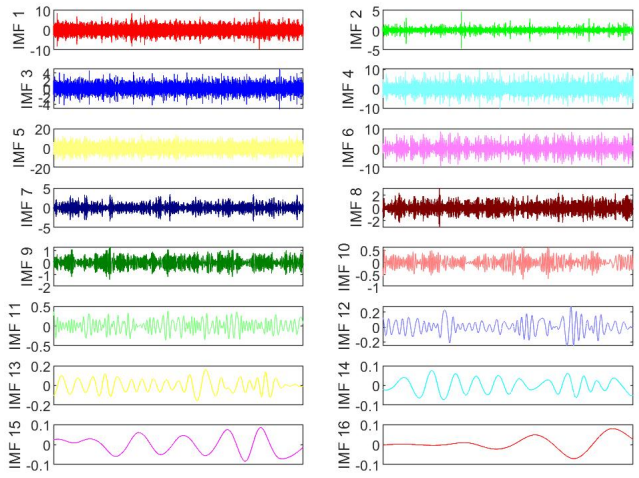

Fig. 6. IMF component.

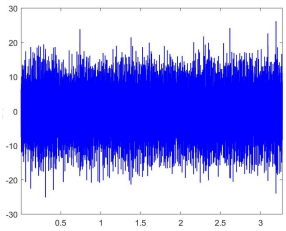

Fig. 7. Signal after noise reduction.

TABLE I. GRCMSE VALUE

Index	IMF1	IMF2	IMF3	IMF4
GRCMSE	1.99	2.33	2.00	1.24
Index	IMF5	IMF6	IMF7	IMF8
GRCMSE	1.27	1.16	1.20	1.03
Index	IMF9	IMF10	IMF11	IMF12
GRCMSE	0.52	0.31	0.26	0.22
Index	IMF13	IMF14	IMF15	IMF16
GRCMSE	0.14	0.07	0.04	0.01

D. Bearing Reliability Modeling

From the vibration signal of the noise-canceled bearing 3-2, 15 features including mean, kurtosis, standard deviation, waveform factor, spectral skewness, spectral kurtosis, and mean square frequency were extracted, covering time domain, frequency domain, and time-frequency domain aspects. Among the time domain features include wavelet packet entropy and singular value factor as shown in Fig. 8. These multi-domain features are combined into a multi-dimensional feature parameter set.

However, directly substituting the multidimensional parameter set into the logistic regression model will bring great

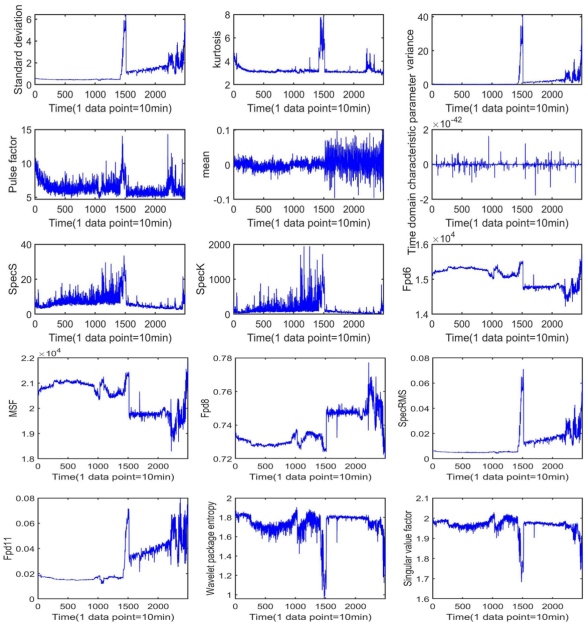

Fig. 8. Multidimensional feature parameter.

challenges, so adopt the UMAP algorithm to reduce the dimensionality of the data features. The core idea of UMAP is to find the local neighborhoods between the data points in the high-dimensional space and find the corresponding neighborhoods in the low-dimensional space, and then try to maintain the relationship between these neighborhoods as much as possible. This approach effectively preserves the local structure of the data and maps it into the low-dimensional space while reducing the dimensionality. And the UMAP is compared with the dimensionality reduction results of PCA and t-SNE to reduce the high-dimensional features to three dimensions. The results after dimensionality reduction are shown in Fig. 9.

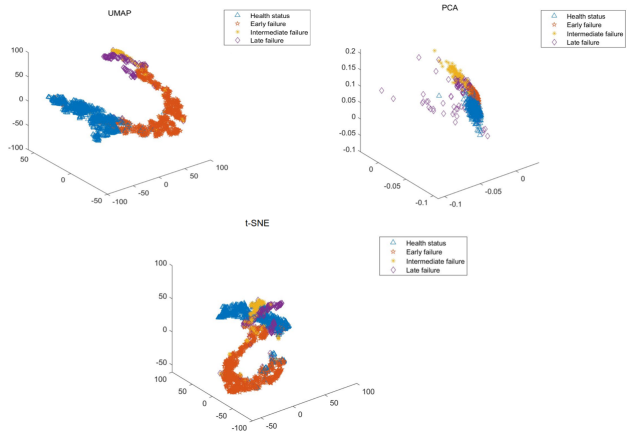

Fig. 9. Dimensionality reduction comparison diagram.

In the figure, it can be observed that different degrees of aliasing exist in the downscaling results of UMAP, PCA and t-SNE algorithms. Especially in the late bearing failure stage, the distribution of data points is more scattered, and there is obvious crossover of data points in different stages. This leads

to a poor differentiation of the bearing operation cycle and fails to clearly reflect the operating condition of the bearing.

In contrast, the UMAP algorithm is able to more clearly delineate the operating cycles of the bearings. The intervals between cycles are more obvious, and the data points in different stages can be well distinguished. This indicates that the dimensionality reduction results of the UMAP algorithm can effectively describe the degradation condition of the bearing.

Through the above processing, the original high-dimensional features are successfully transformed into a more intuitive and easy to understand three-dimensional space which provides a strong foundation for further analysis and modeling.

The set of feature vectors after UMAP dimensionality reduction is selected as the degradation feature information as the parameter of the logistic regression model, and the reliability true curve of 400 points after bearing is obtained as shown in Fig. 10.

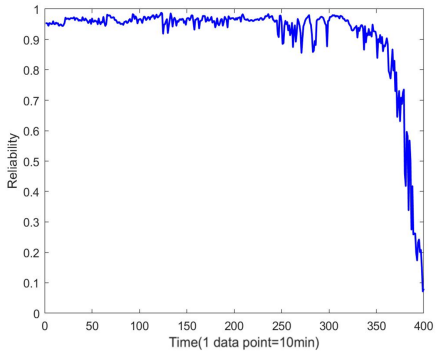

Fig. 10. Bearing reliability real curve.

The next step is to predict the reliability of the bearings, the kernel function of the MKRVM is with the linear kernel function, after many experiments, the performance of the hybrid kernel correlation vector machine reaches the best when the coefficients of the Gaussian kernel are set to 0.6, and the coefficients of the linear kernel are set to 0.4. After RTH optimization, the optimal weight of MKRVM is obtained as 1.327. In order to compare the effectiveness of different optimization algorithms, compared the Red-tailed Hawk algorithm with the Sparrow optimization algorithm and the Particle Swarm optimization algorithm. As shown in Fig. 11 below, it can be clearly observed that the convergence speed of the red-tailed hawk algorithm is much faster than the other two optimization algorithms.

Next, selected the first 2096 data as training data and the last 400 points as test data for the prediction of the RHA-MKRVM model. Subsequently, the final results of RHA-MKRVM were fed into the logistic regression model to obtain the operational reliability of the bearings. We compared the predicted degradation states with the actual data, and the results are shown in Fig. 12.

The final results predicted by the RHA-MKRVM model were incorporated into the logistic regression model, and the regression coefficients were calculated to obtain the operational reliability of the bearings. The comparison between the degraded state of the bearing predicted by the RHA-MKRVM model and the degraded real data is shown in Fig. 13.

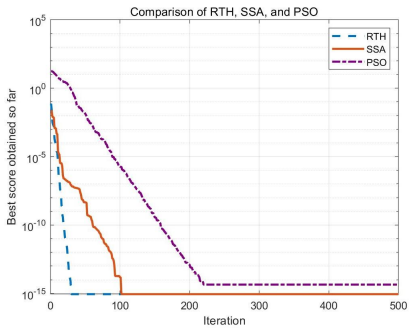

Fig. 11. Effects of different optimization algorithms.

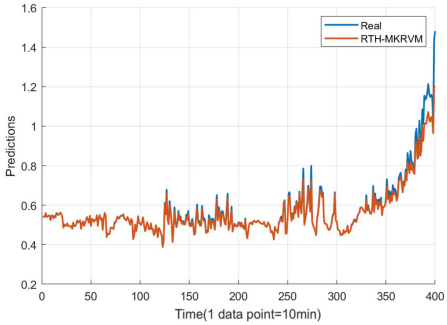

Fig. 12. Bearing degradation state prediction.

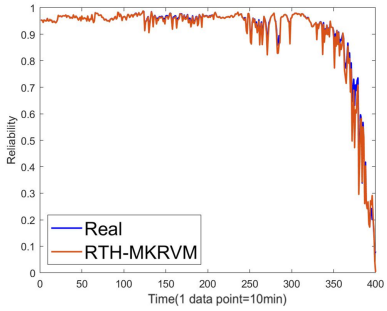

Fig. 13. Bearing reliability prediction.

As can be seen from the above figure, the results predicted by the RHA-MKRVM model are closer to the real situation. In order to verify the prediction accuracy of the hybrid kernel correlation vector machine model, the reliability of the bearings was predicted in this study using the ELMAN neural network, the least squares support vector machine (LSSVM), the correlation vector machine model (RVM), and the hybrid kernel correlation vector machine (MKRVM) model, and the reliability of the bearings was compared with the RTH-MKRVM method.

In LSSVM, Gaussian kernel function is used, and the penalty factor, kernel function parameters are set to 9, 0.002; in ELMAN neural network, the number of neural network layers is set to 3, neuron excitation function is used as Sigmoid function, and the number of neurons in each layer of input,

hidden, and output layers is set to 10, 14, and 1, respectively; in RVM, Gaussian kernel function is used, and the penalty factor, and kernel function parameters are set to 9, 0.002; in MKRVM, Gaussian kernel function and linear kernel are used, and the penalty factor and kernel function parameters are set to 9, 0.002.

The method was also validated using bearing 3-1, bearing 3-4, and bearing vibration data bearing 5 from the University of Cincinnati. The reliability curves for the three bearings are shown in Fig. 14. The errors produced by each prediction model are shown in Table II. From the above figure, it can be seen that the curves obtained by RTH-MKRVM are closer to the actual reliability curves and have good prediction performance compared to the existing bearing reliability prediction methods.

As can be seen in Fig. 14, the early operation of bearing 3-1 was relatively stable, bearing reliability did not change greatly, and there was a serious failure of the bearing at 250 points, and the reliability declined more rapidly. Bearings 3-4 run more smoothly before 300 points, and their reliability drops to 0 in the final stage. Bearing 5 has high reliability before the first 350 points, and after 350 points, reliability suddenly drops to 0.

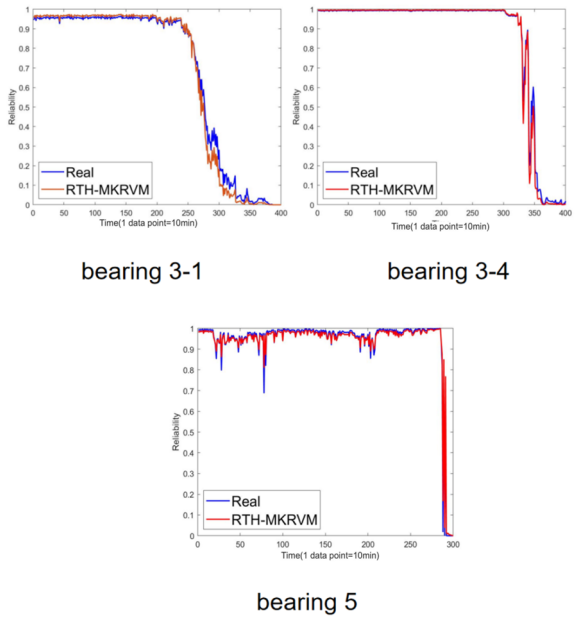

Fig. 14. Three bearing reliability prediction results.

VI. Conclusion

Aiming at the problem of assessing and predicting the reliability of rolling bearings based on noise conditions, a new noise reduction method is proposed to remove the excess noise in the bearing signals, and a logistic regression model is used to assess the reliability of the bearings and obtain the reliability results, and finally a hybrid kernel correlation vector machine model of red-tailed eagle is used to predict the reliability of the bearings, and good results are obtained, indicating that the study can well characterize the rolling bearings' state to characterize and predict the reliability.

TABLE II. Comparison of Different Models on Bearings

Model	Bearing 3-1		Bearing 3-2	
	MAE	MAPE	MAE	MAPE
ELMAN	0.073	0.082	0.032	0.045
LSSVM	0.069	0.074	0.061	0.074
RVM	0.079	0.094	0.135	0.207
MKRVM	0.057	0.041	0.096	0.037
RTH-MKRVM	0.045	0.028	0.058	0.044
Model	Bearing 3-4		Bearing 5	
	MAE	MAPE	MAE	MAPE
ELMAN	0.031	0.072	0.074	0.085
LSSVM	0.074	0.080	0.048	0.066
RVM	0.126	0.209	0.191	0.254
MKRVM	0.029	0.017	0.033	0.027
RTH-MKRVM	0.019	0.026	0.027	0.031

(1) The efficiency of signal noise reduction is greatly improved by combining GRCMSE for the selection problem of IMFs after CEEMDAN.

(2) Use UMAP algorithm to downscale the multidimensional features of the signal after noise reduction, and lay a solid data foundation for the reliability modeling of rolling bearings.

(3) For the problem of bearing reliability prediction, the MKRVM model optimized by the red-tailed eagle algorithm is proposed to predict the reliability of bearing signals, which significantly improves the prediction accuracy.

VII. Discussion

In this paper, the effectiveness of the method is verified by the bearing signal data in the laboratory. However, there are still many problems to be solved in the research of rolling bearings, and the future research direction can be started from the following points:

(1) In terms of bearing signal feature extraction, this paper constructs signal feature set by extracting signal time-frequency domain features, but the selection of signal features also relies on manual experience. In the future research, the selection of signal features can be further studied to make the selection process more automatic, and the selected features can be more accurate representation of the signal.

(2) The verification data used in this paper comes from the laboratory, the working conditions are stable, and the experiment is carried out in an ideal environment. However, the actual operating conditions are complicated, so the reliability assessment and prediction under variable speed conditions should be further studied.

References

[1] T. Andreas,P. Judith, K. Marcel and E. Gordon. "*Predictive maintenance enabled by machine learning: Use cases and challenges in the automotive industry*", Reliability Engineering & System Safety, vol. 215, pp. 107864-107864, 2021.

[2] P. S. Kumar, L. A. Kumaraswamidhas and S. K. Laha, "*Selection of efficient degradation features for rolling element bearing prognosis using Gaussian Process Regression method*", ISA Transactions, vol. 112, pp. 386-401, 2021.

[3] H. Soltanali, A. Rohani, M. Tabasizadeh, M. H. Abbaspour-Fard and A. Parida, "*Operational reliability evaluation based maintenance planning for automotive production line*", Quality Technology & Quantitative Management, vol. 17, no. 2, pp. 1-17, 2020.

[4] S. Bashir, I. M. Kolo, and A. O. S. J. F. "*Development of anomaly detector for motor bearing condition monitoring using fast fourier transform (fft) and long short term memory (lstm)-autoencoder*", -Manager s Journal on Pattern Recognition, vol. 10, no. 1, pp. 1-15, 2023.

[5] Z. Bao, G. Zhang, B. Xiong, et al., "*New image denoising algorithm using monogenic wavelet transform and improved deep convolutional neural network*", Multimedia Tools and Applications, vol. 79, no. 1, pp. 7401–7412, 2020.

[6] X. Zhang, Y. Qi and F. Liu "*Predicting Effects of Non-Point Source Pollution Emission Control Schemes Based on VMD-BiLSTM and MIKE21*", Environmental Modeling & Assessment, vol. 29, pp. 797-812, 2024.

[7] J. Guo, Y. Liu,J. Xiang . "*Rotating Machinery Fault Detection Using a New Version of Intrinsic Time-Scale Decomposition*", IEEE sensors journal, vol. 24, pp. 1905-1918, 2024.

[8] X. Cao, X. Guo, H. Duan , "*Health Status Recognition Method for Rotating Machinery Based on Multi-Scale Hybrid Features and Improved Convolutional Neural Networks*", sensors, vol. 12, pp. 5688, 2023.

[9] N. E. Huang, Z. Shen, S. R. Long, M. C. Wu, H. H. Shih, Q. Zheng, N.-C. Yen, C.-C. Tung and H. H. Liu, "*The empirical mode decomposition and the Hilbert spectrum for nonlinear and non-stationary time series analysis*", Proceedings of the Royal Society A: Mathematical, Physical & Engineering Sciences, vol. 454, no. 1971, pp. 903-995, 1998.

[10] J. Zheng and H. Pan, "*Mean-optimized mode decomposition: An improved EMD approach for non-stationary signal processing*", ISA transactions, vol. 106,pp. 392-401, 2020.

[11] L. Zhao, Z. Li,Y. Pei, "*Disentangled Seasonal-Trend representation of improved CEEMD-GRU joint model with entropy-driven reconstruction to forecast signicant wave height*", Renewable Energy, vol. 226, pp.120345, 2024.

[12] M. E. Torres, M. A. Colominas, G. Schlotthauer and P. Flandrin, "*A complete ensemble empirical mode decomposition with adaptive noise*", IEEE International Conference on Acoustics, Speech and Signal Processing, pp. 4144–4147, 2011.

[13] Y. Cheng, Z. Wang, B. Chen, W. Zhang and G. Huang, "*An improved complementary ensemble empirical mode decomposition with adaptive noise and its application to rolling element bearing fault diagnosis*", ISA Transactions, vol. 19, pp. 218–234, 2019.

[14] A. Kala, S. Vaidyanathan and P. Femi, "*Ceemdan hybridized with lstm model for forecasting monthly rainfall*", Journal of Intelligent & Fuzzy Systems: Applications in Engineering and Technology, vol. 43, pp. 1–9, 2022.

[15] J. Zhang, Z. Li and J. Huang, "*Study on vibration-transmission-path identification method for hydropower houses based on ceemdan-svd-te*", Applied Sciences, vol. 12, pp. 7455, 2022.

[16] Y. Zhao and J. Xu, "*Denoising of ECG signals based on CEEMDAN*", 2021 6th International Conference on Intelligent Computing and Signal Processing (ICSP), pp. 430–433, 2022.

[17] M. Ding and X. Wang, "*Indirect prediction method for remaining useful life of lithium-ion battery based on gray wolf optimized extreme learning machine*", 2023 IEEE 12th Data Driven Control and Learning Systems Conference (DDCLS), pp. 301–306, 2023.

[18] M. Jürgen, H P. Gnser,W. Daves, "*Digitalization and Reliability of Railway Vehicles and Tracks—Condition Monitoring and Condition-based Maintenance*", BHM Berg- und Hüttenmännische Monatshefte, vol.169, pp.264-268, 2024.

[19] S. Gao, S. Zhang, Y. Zhang and Y. Gao, "*Operational reliability evaluation and prediction of rolling bearing based on isometric mapping and NOCUSa-LSSVM*", Reliability Engineering & System Safety, vol. 201, pp. 106968.1–106968.11, 2020.

[20] F. Abbasi, M. Naderan and S. E. Alavi, "*Anomaly detection in Internet of Things using feature selection and classification based on Logistic Regression and Artificial Neural Network on N-BaIoT dataset*", 2021 5th International Conference on Internet of Things and Applications (IoT), pp.1-7, 2021.

[21] Q. Li, M. J. Zuo and S. Y. Liang, "*False Lipschitz penalty sparse low-rank matrix and chaotic bionic optimization for prognosis of bearing degradation*", IEEE Transactions on Reliability, pp. 1–17, 2020.

[22] T. Han, J. Pang and A. C. Tan, "*Remaining useful life prediction of bearing based on stacked autoencoder and recurrent neural network*", Journal of Manufacturing Systems, vol. 21, pp. 576–591, 2021.

[23] Y. Wang, J. Zhao, C. Yang, D. Xu and J. Ge, "*Remaining useful life prediction of rolling bearings based on Pearson correlation-KPCA multi-feature fusion*", Measurement, vol. 20, pp. 111572, 2022.

[24] Z. Xu, M. Bashir, Q. Liu, Z. Miao, X. Wang, J. Wang and N. Ekere, "*A novel health indicator for intelligent prediction of rolling bearing remaining useful life based on unsupervised learning model*", Computers & Industrial Engineering, vol. 176, pp. 108999, 2023.

[25] B. Su and Y. Sun, "*Intelligent prediction of bearing remaining useful life based on data enhancement and adaptive temporal convolutional networks*", Journal of Failure Analysis and Prevention, vol. 23, pp. 2709–2720, 2023.

[26] J. S. Richman and J. R. Moorman, "*Physiological time-series analysis using approximate entropy and sample entropy*", American Journal of Physiology Heart & Circulatory Physiology, vol. 278, pp. H2039–H2049, 2000.

[27] B. Ghojogh, M. Crowley, F. Karray and A. Ghodsi, "*UMAP: Uniform manifold approximation and projection for dimension reduction*", The Journal of Open Source Software, pp. 479–497, 2023.

[28] J. Shlens, "*A tutorial on principal component analysis*", International Journal of Remote Sensing, vol. 51, 2014.

[29] D. R. Cox, "*Regression models and life-tables*", Journal of the Royal Statistical Society, vol. 34, pp. 527–541, 1972.

[30] S. Ferahtia, A. Houari, H. Rezk and A. Djerioui, "*Red-tailed hawk algorithm for numerical optimization and real-world problems*", Scientific Reports, vol. 13, pp. 12950, 2023.

[31] P. E. Tipping, "*Sparse Bayesian learning and the relevance vector machine*", Journal of Machine Learning Research, vol. 1, pp. 211–224, 2001.